

Note

A note on graphite hydrogenation as a source of abiotic methane on rocky planets: A case study for Mercury

Camille R. Butkus^{a,1}, Alexandra O. Warren^b, Edwin S. Kite^b, Santiago Torres^{c,d}, Smadar Naoz^{c,d}, Jennifer B. Glass^{e,*}

^a School of Civil and Environmental Engineering, Georgia Institute of Technology, Atlanta, GA, USA

^b Department of the Geophysical Sciences, University of Chicago, Chicago, IL, USA

^c Department of Physics & Astronomy, University of California Los Angeles, Los Angeles, CA, USA

^d Mani L. Bhaumik Institute for Theoretical Physics, Department of Physics and Astronomy, University of California Los Angeles, Los Angeles, CA, USA

^e School of Earth and Atmospheric Sciences, Georgia Institute of Technology, Atlanta, GA, USA



ARTICLE INFO

Keywords:

Astrobiology

Mercury, surface

Search for extraterrestrial life

ABSTRACT

Methane is a promising gaseous biosignature on rocky exoplanets, given a suitable context. Establishing the robustness of methane biosignatures on rocky exoplanets requires assessing potential “false positive” production pathways that could yield large fluxes of methane of abiotic origin. Here we modeled the flux of abiotic methane production from graphite hydrogenation on the surface of Mercury, where a relatively carbon-rich crust and bombardment by solar protons might favor this reaction. We calculated negligible methane flux from this abiotic reaction compared to biological methane flux on Earth. Graphite hydrogenation would only be expected to yield significant methane fluxes on exoplanets with high temperatures and ion fluxes that would preclude habitability for life as we know it. Thus, graphite hydrogenation by stellar wind can likely be ruled out as a potential “false positive” methane biosignature source.

1. Introduction

Methane may be detectable in the atmospheres of terrestrial exoplanets with the new generation of space telescopes (Krissansen-Totton et al., 2018a; Thompson et al., 2022). On Earth, methane is mainly produced by microbial methanogenesis in anoxic environments and thermal breakdown of ancient organic matter, with minor fluxes from magmatic and hydrothermal activity (Etiope et al., 2013; Guzman-Marmolejo et al., 2013; Reeves and Fiebig, 2020). On exoplanets, the ratios of methane to carbon monoxide and carbon dioxide aid in determining if methane has biotic or abiotic origins (Krissansen-Totton et al., 2018b). Atmospheres with high levels of methane and carbon dioxide but low levels of carbon monoxide are most consistent with biological processes (Thompson et al., 2022). Additionally, carbon monoxide can be readily consumed by microorganisms for energy, indicating that low atmospheric levels of carbon monoxide are more consistent with the presence of life (Krissansen-Totton et al., 2022). Thus, co-existence of methane and carbon dioxide, with minimal carbon monoxide, has been proposed to be a particularly robust gaseous

biosignature on terrestrial exoplanets (Krissansen-Totton et al., 2022; Wogan et al., 2020). However, a common assumption in previous models of methane production is that the terrestrial planet’s crustal composition is similar to that of Earth; Earth’s crustal C content is greatly depleted due to the stellar C/O ratio as a result of a complex series of processes that would not necessarily occur and/or lead to the same degree of C depletion on exoplanets (Hakim, 2019; Kim, 2022), for example stochastic accretion (Bergin et al., 2015; Li et al., 2016). An unexplored abiotic methane production pathway on carbon-rich exoplanets is hydrogenation of graphite, likely the dominant mineral phase of carbon in the planet’s crust.

2. Graphite hydrogenation as a source of abiotic methane

Graphite hydrogenation is the process whereby carbon atoms are eroded by and become saturated with hydrogen, either as hydrogen gas (H₂) or hydrogen ions (H⁺), to produce methane (CH₄) or other hydrocarbons (Eq. (1)):

* Corresponding author at: Georgia Tech School of Earth and Atmospheric Sciences, 311 Ferst Drive, Atlanta, GA 30332-0340, USA.

E-mail address: jennifer.glass@eas.gatech.edu (J.B. Glass).

¹ Present address: Department of Geology & Environmental Science, University of Pittsburgh, Pittsburgh, PA, USA.



Numerous studies have characterized the rates and mechanisms of graphite hydrogenation by H^+ ions. Most of these studies were motivated by work on tokamaks, devices containing plasma inside of a chamber where hydrogenation can degrade the graphite tile walls and cause unwanted accumulation of methane gas (Davis et al., 1987; Haasz and Davis, 2004; Haasz et al., 1987). Methane was found to be either the dominant hydrocarbon or the sole hydrocarbon produced by the reaction of graphite by H^+ plasmas in tokamaks (Bernardo and Trimm, 1979; Breisacher and Marx, 1963; Dziembaj et al., 1996; Goethel and Yang, 1987; Roth and García-Rosales, 1996; Rye, 1977). Roth and García-Rosales (1996) parameterized these experimental results into equations (see Supplemental Data) to determine how much carbon erosion is expected based on ion energy (E_0), ion flux (ϕ), and reaction temperature (T). These equations were derived empirically from experiments performed at 1–1000 eV, 10^{18} – $10^{20} \text{ H}^+ \text{ m}^{-2} \text{ s}^{-1}$, and 300–1400 K for E_0 , ϕ , and T , respectively (Roth, 1999; Roth and García-Rosales, 1996).

3. Case study: graphite hydrogenation on Mercury

Mercury has favorable conditions for graphite hydrogenation, including ample hydrogen ions supplied by solar winds (Zurbuchen et al., 2011) and compelling evidence for a relatively graphite-rich crust (Peplowski et al., 2016). Mercury's surface is also scattered with shallow craters, or hollows (Blewett et al., 2011). Graphite hydrogenation by bombardment with solar protons was proposed by Blewett et al. (2016) as a potential formation mechanism for Mercury's hollows. Here, we used the equations developed by Roth and García-Rosales (1996) (see Supplemental Data) to calculate the estimated yield of methane from graphite hydrogenation on Mercury. Supplemental eqs. 2 to 10 were evaluated using published data on solar protons striking Mercury's surface with 100–2000 eV (Zurbuchen et al., 2011), at a rate of 10^8 – $10^{13} \text{ H}^+ \text{ m}^{-2} \text{ s}^{-1}$ (Kallio et al., 2008), over Mercury's 90–700 K temperature range (Vasavada et al., 1999). Maximum methane ($\sim 8 \bullet 10^{25} \text{ C atoms s}^{-1}$) is produced at $\sim 350 \text{ eV}$, $10^{13} \text{ H}^+ \text{ m}^{-2} \text{ s}^{-1}$, and $\sim 500 \text{ K}$ (Fig. 1).

Four major assumptions were used in our calculations. First, we assumed that the equations developed by Roth and García-Rosales (1996) hold true at planetary conditions applicable to Mercury (Table 1). Second, we assumed that the entire surface of Mercury is covered in graphite; in reality, Mercury's surface is dominated by igneous minerals (FeO-poor pyroxene and olivine, and plagioclase) and Mg-Ca-Fe-sulfides, and the amount of carbon is only a few weight

Table 1

Variables and applicable ranges used to calculate methane production via graphite hydrogenation on Mercury.

Parameter	Definition	Experimental ¹	Mercury ^{2,3,4}	Unit
E_0	Ion energy	1–1000	100–2000	eV
ϕ	Ion flux	10^{18} – 10^{20}	10^8 – 10^{13}	$\text{H}^+ \text{ m}^{-2} \text{ s}^{-1}$
T	Temperature	300–1400	90–700	K

Source: ¹Roth (1999), ²Zurbuchen (2011), ³Kallio et al. (2008), ⁴Vasavada et al. (1999).

percent (Nittler and Weider, 2019), so, our calculation is a conservative upper bound. Third, we assumed that graphite erosion of one carbon atom produces one methane molecule. Methane does indeed dominate the products of this reaction (Bernardo and Trimm, 1979; Breisacher and Marx, 1963; Dziembaj et al., 1996; Goethel and Yang, 1987; Roth and García-Rosales, 1996; Rye, 1977). In reality, other minor CH_n products are also formed (Busharov et al., 1976; Erents et al., 1976). Moreover, temperature-dependent diffusion of methane to the surface of the graphite lattice may limit its release from graphite (Roth and Bohdansky, 1987). Thus, our assumption of 100% efficiency is an overestimate by up to two orders of magnitude, again providing a conservative upper bound. Our fourth assumption was that solar wind is 100% protons, whereas it is in fact 95% H^+ , 4% He^{++} , and 1% minor ions (Ogilvie and Coplan, 1995).

4. Discussion

To better understand the magnitude of methane yield for this scenario, we compared it to approximate methane fluxes on Mars and Earth

Table 2

Approximate methane fluxes on Mercury, Mars, and Earth.

Planet/process	Estimated methane flux ($\text{mmol m}^{-2} \text{ yr}^{-1}$)
Mercury	0.06
Mars ¹	0.000004
Earth ²	60
Serpentinization	0.04
Volcanic outgassing	0.002

¹ The flux here is to produce a mean global concentration of 0.4 ppbv (Lefevre and Forget, 2009; Webster, 2021), noting that this may be an overestimate (Montmessin, 2021).

² Thompson et al. (2022).

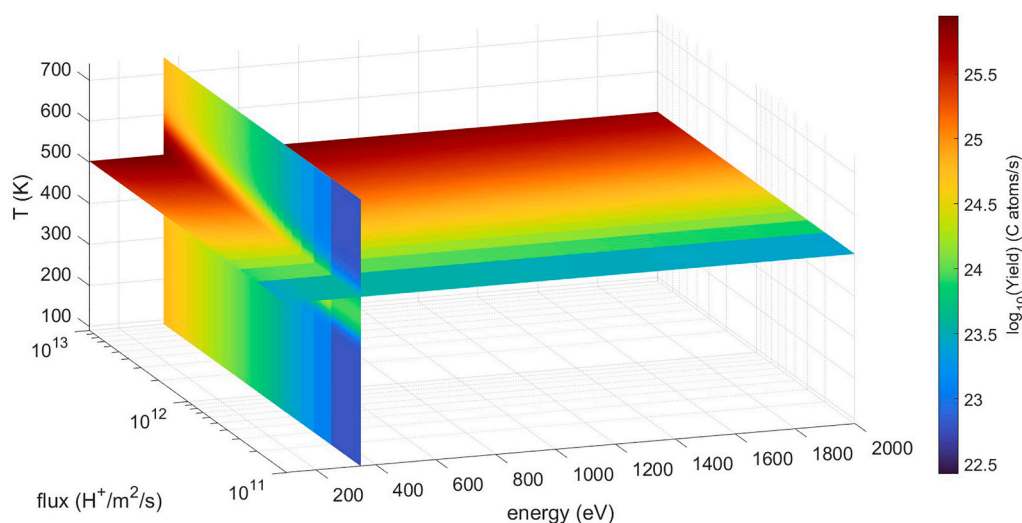


Fig. 1. Carbon erosion calculated for graphite hydrogenation on Mercury as a function of temperature, ion energy, and ion flux. Horizontal slice shows conditions where the largest amount of methane is produced.

(Table 2), noting that some instruments at Mars, such as those from ESA's Trace Gas Orbiter, detect no methane at all (Montmessin et al., 2021). Our maximum value for methane production from graphite hydrogenation on Mercury ($0.06 \text{ mmol m}^{-2} \text{ yr}^{-1}$) is similar to the methane flux estimated for Earth from the abiotic process of H_2 production from serpentinization followed by Fischer-Tropsch reduction of carbon, $0.04 \text{ mmol m}^{-2} \text{ yr}^{-1}$ (Thompson et al., 2022). However, because we assumed Mercury's surface is entirely covered in graphite, our approximation is likely an overestimate of methane production. This comparison implies that graphite hydrogenation is unlikely to create a large flux of abiotic methane on Mercury.

Graphite hydrogenation has been proposed as a mechanism for hollows formation on Mercury (Blewett et al., 2016). Proton flux supplied by solar winds may have been up to ~ 60 times higher in the past, a factor obtained by dividing the relative mass loss rate of the Sun at an age of $7 \cdot 10^8$ years ($\sim 1 \cdot 10^{-12} M_{\text{Sun}} \text{ yr}^{-1}$) by the solar mass loss rate measured by space experiments ($2 \cdot 10^{-14} M_{\text{Sun}} \text{ yr}^{-1}$) (Linsky et al., 2011). Integrating the mass loss rate of the Sun from 0.7 to 4.5 Gy age, we find that proton flux may have been up to ~ 10 times higher in the past, on average (Supplemental Data, Eq. 12). Translating to conditions on Mercury, a minimum for proton flux at a low point in the solar cycle when the Sun was young ($10^9 \text{ H}^+ \text{ m}^{-2} \text{ s}^{-1}$) and maximum proton flux ($10^{14} \text{ H}^+ \text{ m}^{-2} \text{ s}^{-1}$) were used to estimate a maximum methane yield of $9 \cdot 10^{26} \text{ C atoms s}^{-1}$ (Supplemental Data, Eq. 2 to 10). Again, this approach provides a conservative upper bound of methane production on Mercury if it were to be fully covered in graphite. This maximum methane yield, which accounts for changes in proton flux over time, translates to at most ~ 14 m of ablation over the lifetime of Mercury (~ 4 Gy; Supplemental Data, Eq. 14). With mean depths of hollows found to be 24 m, graphite hydrogenation may partially contribute to their formation on Mercury (Blewett et al., 2016). An additional mechanism for the formation of Mercury's hollows could be reactions between minerals and reduced sulfur gases (Barraud et al., 2023; Renggli et al., 2022).

Methane yields may be higher in the presence of transition metal catalysts, including common crustal elements such as nickel (Goethel and Yang, 1987; Kelley and Goodman, 1982), calcium (Casanova et al., 1983), and potassium (Casanova et al., 1983). Other studies have compared methane yields in the presence of different transition metal catalysts and low-temperature aqueous fluid. Metals ranked in order of most to least increase in methane yields were found to be $\text{Rh} \geq \text{Ru} \geq \text{Ir} > \text{Pt} > \text{Ni} \gg \text{Pd} \geq \text{Co} \geq \text{Fe}$ (Tomita and Tamai, 1972) and similarly $\text{Ni} > \text{Co} \gg \text{Fe}$ (Dziembaj et al., 1996).

The ion flux on Mercury is several orders of magnitude lower when compared to Roth (1999)'s experimental values, which is a potential source of error in the calculated methane yields. Conducting experiments in the appropriate ion flux ranges is necessary to support or refute the applicability of Roth's equations under low H^+ fluxes and to quantify methane yields under such conditions.

Moreover, to achieve high proton fluxes at its surface and have high temperatures to support graphite hydrogenation, an exoplanet must be close to its star and have a thin or nonexistent atmosphere. However, thin atmospheres are more vulnerable to atmospheric escape and, therefore, less likely to persist (Kreidberg et al., 2019). Conversion of graphite to methane would also deplete the near-surface of graphite, potentially leaving a graphite-poor lag deposit and curtailing methane production unless resurfacing by fresh graphite-rich material frequently occurred.

5. Conclusions

Applying environmental conditions of Mercury to available analytical equations for graphite hydrogenation predicts a low methane flux. Additionally, conditions that favor higher amounts of graphite hydrogenation are uninhabitable. Methane produced from this reaction is not likely to cause a false biosignature for our example case study on Mercury. However, additional experimental data of graphite hydrogenation

under planetary conditions, specifically low H^+ flux, is necessary to accurately estimate methane production from this reaction. Additional factors to consider include the presence of metal catalysts and habitability of a planet that would require consideration of biosignatures. More work is required to understand planetary conditions different than Earth and the reactions that may occur there to produce false positives for biosignatures.

Declaration of Competing Interest

The authors declare that they have no known competing financial interests or personal relationships that could have appeared to influence the work reported in this paper.

Data availability

No data was used for the research described in the article.

Acknowledgements

We thank Joachim Roth for helpful comments and insight on graphite hydrogenation. We thank David Catling for detailed reviewer feedback. Financial support for this publication results from a Scialog program sponsored jointly by Research Corporation for Science Advancement (RCSA) and the Heising-Simons Foundation and includes a grant (#28094) to Georgia Tech Research Corporation by RCSA, a grant (#28116) to the University of Chicago by RCSA, and a grant (#28090) to the University of California, Los Angeles by RCSA.

Appendix A. Supplementary data

Supplementary data to this article can be found online at <https://doi.org/10.1016/j.icarus.2023.115580>.

References

- Barraud, O.A., Besse, S.B., Doressoundiram, A., 2023. Low sulfide concentration in Mercury's smooth plains inhibits hollows. *Sci. Adv.* 9, eadd6452.
- Bergin, E.A., Blake, G.A., Ciesla, F., Hirschmann, M.M., Li, J., 2015. Tracing the ingredients for a habitable earth from interstellar space through planet formation. *Proc. Natl. Acad. Sci.* 112, 8965–8970.
- Bernardo, C.A., Trimm, D.L., 1979. The kinetics of gasification of carbon deposited on nickel catalysts. *Carbon* 17, 115–120.
- Blewett, D.T., et al., 2011. Hollows on Mercury: MESSENGER evidence for geologically recent volatile-related activity. *Science* 333, 1856–1859.
- Blewett, D.T., et al., 2016. Analysis of MESSENGER high-resolution images of Mercury's hollows and implications for hollow formation. *J. Geophys. Res. Planets* 121, 1798–1813.
- Breisacher, P., Marx, P.C., 1963. The hydrogen-graphite reaction between 360 and 800°. *J. Am. Chem. Soc.* 85, 3518–3519.
- Busharov, N.P., Gorbatov, E.A., Guseva, V.M., Guseva, M.I., Martynenko, Y.V., 1976. Chemical sputtering of graphite by H^+ ions. *J. Nucl. Mater.* 63, 230–234.
- Casanova, R., Cabrera, A.L., Heinemann, H., Somorjai, G.A., 1983. Calcium oxide and potassium hydroxide catalysed low temperature methane production from graphite and water comparison of catalytic mechanisms. *Fuel* 62, 1138–1144.
- Davis, J.W., Haasz, A.A., Stangeby, P.C., 1987. Flux and energy dependence of methane production from graphite due to H^+ impact. *J. Nucl. Mater.* 145–147, 417–420.
- Dziembaj, R., Makowski, W., Chmielarz, L., 1996. Synergistic effects in the transition metal catalysed hydrogenation of commercial graphites promoted by $\text{Ca}(\text{NO}_3)_2$ and pretreated with O_2 or CO_2 . *Carbon* 34, 913–916.
- Erents, S.K., Braganza, C.M., McCracken, G.M., 1976. Methane formation during the interaction of energetic protons and deuterons with carbon. *J. Nucl. Mater.* 63, 399–404.
- Etiopie, G., Ehlmann, B.L., Schoell, M., 2013. Low temperature production and exhalation of methane from serpentinized rocks on Earth: a potential analog for methane production on Mars. *Icarus* 224, 276–285.
- Goethel, P.J., Yang, R.T., 1987. Mechanism of graphite hydrogenation catalyzed by nickel. *J. Catal.* 108, 356–363.
- Guzman-Marmolejo, A., Segura, A., Escobar-Briones, E., 2013. Abiotic production of methane in terrestrial planets. *Astrobiology* 13, 550–559.
- Haasz, A.A., Davis, J.W., 2004. Erosion of carbon in dual-beam experiments: an overview. *Phys. Scr.* T111, 68.
- Haasz, A.A., et al., 1987. Synergistic methane formation on pyrolytic graphite due to combined H^+ ion and H^0 atom impact. *J. Nucl. Mater.* 145–147, 412–416.

- Hakim, K., et al., 2019. Mineralogy, structure, and habitability of carbon-enriched rocky exoplanets: a laboratory approach. *Astrobiology* 19, 867–884.
- Kallio, E., et al., 2008. On the impact of multiply charged heavy solar wind ions on the surface of Mercury, the moon and Ceres. *Planet. Space Sci* 56, 1506–1516.
- Kelley, R., Goodman, D.W., 1982. Catalytic methanation over single crystal nickel and ruthenium: reaction kinetics on different crystal planes and the correlation of surface carbide concentration with reaction rate. *Surf. Sci. Lett.* 123, L743–L749.
- Kim, D., et al., 2022. Structure and density of silicon carbide to 1.5 TPa and implications for extrasolar planets. *Nat. Commun.* 13, 2260.
- Kreidberg, L., et al., 2019. Absence of a thick atmosphere on the terrestrial exoplanet LHS 3844b. *Nature* 573, 87–90.
- Krissansen-Totton, J., Garland, R., Irwin, P., Catling, D.C., 2018a. Detectability of biosignatures in anoxic atmospheres with the James Webb space telescope: a TRAPPIST-1e case study. *Astron. J.* 156, 114.
- Krissansen-Totton, J., Olson, S., Catling, D.C., 2018b. Disequilibrium biosignatures over earth history and implications for detecting exoplanet life. *Sci. Adv.* 4, eaao5747.
- Krissansen-Totton, J., Thompson, M., Galloway, M.L., Fortney, J.J., 2022. Understanding planetary context to enable life detection on exoplanets and test the Copernican principle. *Nat. Astron.* 6, 189–198.
- Lefevre, F., Forget, F., 2009. Observed variations of methane on Mars unexplained by known atmospheric chemistry and physics. *Nature* 460, 720–723.
- Li, Y., Dasgupta, R., Tsuno, K., Monteleone, B., Shimizu, N., 2016. Carbon and sulfur budget of the silicate earth explained by accretion of differentiated planetary embryos. *Nat. Geosci.* 9, 781–785.
- Linsky, J.L., Wood, B.E., Redfield, S., 2011. The solar wind in time. *Proc. Int. Astronom. Union* 7, 286–290.
- Montmessin, F., et al., 2021. A stringent upper limit of 20 pptv for methane on Mars and constraints on its dispersion outside Gale crater. *Astron. Astrophys.* 650, A140.
- Nittler, L.R., Weider, S.Z., 2019. The surface composition of mercury. *Elements* 15, 33–38.
- Ogilvie, K.W., Coplan, M.A., 1995. Solar wind composition. *Rev. Geophys.* 33, 615–622.
- Peplowski, P.N., et al., 2016. Remote sensing evidence for an ancient carbon-bearing crust on Mercury. *Nat. Geosci.* 9, 273–276.
- Reeves, E.P., Fiebig, J., 2020. Abiotic synthesis of methane and organic compounds in Earth's lithosphere. *Elements* 16, 25–31.
- Renggli, C.J., et al., 2022. Sulfides and hollows formed on Mercury's surface by reactions with reducing S-rich gases. *Earth Planet. Sci. Lett.* 593, 117647.
- Roth, J., 1999. Chemical erosion of carbon based materials in fusion devices. *J. Nucl. Mater.* 266-269, 51–57.
- Roth, J., Bohdanský, J., 1987. Mechanism of hydrocarbon formation upon interaction of energetic hydrogen ions with graphite. *Appl. Phys. Lett.* 51, 964–966.
- Roth, J., García-Rosales, C., 1996. Analytic description of the chemical erosion of graphite by hydrogen ions. *Nucl. Fusion* 36, 1647–1659.
- Rye, R.R., 1977. Reaction of thermal atomic hydrogen with carbon. *Surf. Sci.* 69, 653–667.
- Thompson, M.A., Krissansen-Totton, J., Wogan, N., Telus, M., Fortney, J.J., 2022. The case and context for atmospheric methane as an exoplanet biosignature. *Proc. Natl. Acad. Sci.* 119, e2117933119.
- Tomita, A., Tamai, Y., 1972. Hydrogenation of carbons catalyzed by transition metals. *J. Catal.* 27, 293–300.
- Vasavada, A.R., Paige, D.A., Wood, S.E., 1999. Near-surface temperatures on mercury and the moon and the stability of polar ice deposits. *Icarus* 141, 179–193.
- Webster, C.R., et al., 2021. Day-night differences in Mars methane suggest nighttime containment at Gale crater. *Astron. Astrophys.* 650, A166.
- Wogan, N., Krissansen-Totton, J., Catling, D.C., 2020. Abundant atmospheric methane from volcanism on terrestrial planets is unlikely and strengthens the case for methane as a biosignature. *Planet. Sci. J.* 1, 58.
- Zurbuchen, T.H., et al., 2011. MESSENGER observations of the spatial distribution of planetary ions near Mercury. *Science* 333, 1862–1865.